B. G. Huth

Calculations of Stable Domain Radii Produced by Thermomagnetic Writing

Abstract: Calculations are performed to determine the stable radius of a cylindrically symmetric domain nucleated in magneto-optical films during thermomagnetic writing with a laser beam. A critical bound on domain size is calculated which determines whether or not a domain of given radius, once nucleated, will be stable. The analysis shows that for a ferromagnetic material such as MnAlGe, the domain dimensions can grow beyond the local region of material that is heated above the Curie temperature. For ferrimagnetic thin films having a compensation point, T_{comp}, stability depends on the difference between ambient and compensation temperatures, $\Delta T = T_a - T_{comp}$. With $\Delta T \approx 0$, wall energy dominates and the critical radius can be calculated from $R_c = \sigma/(2MH_c)$.

Introduction

Recent experiments on thermomagnetic writing with lasers on ferromagnetic magneto-optic materials have shown that switching of the local magnetization can occur at temperatures lower than the Curie temperature [1-3]. When the coercivities are low at temperatures close to the Curie temperature, the switched spots can grow and encompass areas larger than those actually heated above the Curie point. Predicting the size of reversed spots now becomes more complex than in the case of true Curie-point writing, and the magnetic forces tending to expand or contract the thermally nucleated domain must be considered. Similar considerations of the forces are also important for thermomagnetic writing on ferrimagnetic materials having compensation points, such as GdIG or GdCo. In this paper we calculate these forces on the cylindrically symmetrical Bloch-domain wall surrounding a thermomagnetically written "bit" of reverse-magnetized material and determine the ranges of bit radius for which a stable domain exists.

The analysis that follows is based on a bubble-type approach such as given by Bobeck and by Thiele [4]. To describe the bit, the simple magnetic bubble model must be modified for two reasons: 1) The intrinsic magnetization within the bit varies with distance from the center because of the laser beam intensity profile, and 2) the wall-motion coercivity is not negligibly small. The domain-wall stability is not determined simply by a balance between strictly conservative forces, as is the case for the conventional magnetic bubble, but results instead from the inability of those forces to overcome the local coercive potential.

The analysis and calculations performed here are based on a specific set of assumptions:

1. The stability theory in this work is derived from a quasistatic process rather than a dynamic process.
2. The stability calculation deals with *radial* stability for bubbles created by the laser beam, whereas bubbles may normally suffer elliptical instability as well.
3. Beam heating is assumed to penetrate the film material uniformly, and the temperature profile contains no dependence on the z coordinate.
4. The calculations here pertain to pure Bloch walls.

Other bubble-type calculations directed toward thermomagnetically written bits have appeared in the literature. Schuldt and Chen [5] considered the stability of bubbles in MnBi with an assumed wall coercivity of 250 Oe. They assumed a uniform temperature throughout the film and calculated the maximum field that could be applied in the erase direction without reducing domain size. Knowledge of this critical field is important for the selective erasure of information stored magneto-optically, since an excessively large erase field would reduce the readout signal from all the stored bits.

Esho et al. [6] performed a similar analysis. In addition, their experiments showed that the wall coercivity

for MnBi decreased linearly with increasing film thickness. By including this behavior for the coercivity in their analysis, they concluded that MnBi films should be less than 700 Å thick to prevent inadvertent signal loss during erasure.

Neither of these two analyses, however, considered the effects on the wall forces produced by a laser-produced temperature distribution in the magnetic thin film. The main purpose of this paper is to calculate the region of stable domain radii in the presence of a Gaussian thermal profile and to provide insight into the sizes of the domains produced by thermomagnetic writing.

The equations used in the analysis are developed in the next section. Then the results of numerical calculations are presented for one ferromagnetic and one ferrimagnetic material having a compensation point. The parameters of the ferromagnet are typical of MnAlGe [7], and those for the ferrimagnet are representative of GdCo [8].

Analysis of stable domain size

At ambient temperature the material is assumed to have uniform magnetic properties and to have sufficient uniaxial anisotropy to support magnetization normal to the plane. We assume that at some instant of time the laser produces a cylindrically symmetric Gaussian distribution of temperature throughout the thickness of the magnetic thin film. This local heating nucleates the reversed domain. Details of the nucleation process, however, are not considered here.

The calculations of equilibrium domain size (which is reached after the temperature profile is established) begin in the same manner as those of Bobeck for the magnetic bubble. We assume that a bubble is already present in the thin film and proceed to calculate the radial forces on the domain wall. The total energy, E_t, of a reversed cylindrical domain in a film uniformly saturated downward relative to the same film without a reversed region is given by

$$E_t = 2\pi R h \sigma_w(R) - \xi_d(R) - 4\pi h H_a \int_0^R M(\rho)\rho d\rho, \quad (1)$$

where $\sigma_w(R)$ is the domain-wall energy per unit area in ergs/cm^2, and $\xi_d(R)$ is the magnetostatic, self-demagnetizing energy arising from the distribution itself in the thin film of thickness h. If the radial coordinate is indicated by r, it is assumed that the domain wall is positioned at $r = R$, and a dummy variable, ρ, is used in the integral term arising from the interaction between the magnetization and the external bias field, H_a. An integral is necessary because of the spatial variation in magnetization produced by the laser-produced temperature profile. In the sign convention adopted, the unswitched magnetization is negative and, hence, external biases that aid in thermomagnetic switching (i.e., "write bias") are positive in sign.

The force on the domain wall may be found by differentiating the total energy with respect to the domain radius, R,

$$\frac{\partial E_t}{\partial R} = 2\pi h \sigma_w(R) + 2\pi R h[(\partial\sigma_w(R)/\partial R) - (\partial\xi_d(R)/\partial R)] - 4\pi R h H_a |M(R)|. \quad (2)$$

Although the usual assumption for bubbles is that σ_w is explicitly independent of the wall curvature [4], we note that, in general, the wall energy is a function of temperature and, therefore, must depend implicitly on radius. The term $\partial\xi_d(R)/\partial R$ is related to the demagnetizing field (evaluated at the domain wall) which is averaged over the z coordinate [4]. A more detailed discussion of this z-averaged demagnetizing field, $\overline{H}_d(R)$, is given in Appendix B, and the result is

$$\partial\xi_d(R)/\partial R = 4\pi R h \overline{H}_d(R)|M(R)|. \quad (3)$$

The positive terms in Eq. (2) tend to shrink the reversed domain, and the negative terms tend to expand it. Note that the effect of the external bias field is opposite to the conventional bubble case.

The stability condition of usual interest in bubble materials occurs when the force given in Eq. (2) is exactly zero [4]. Thus a stable domain can exist even in the absence of a wall coercivity. On the other hand, in magneto-optic materials for application to beam-addressable storage, large coercivities are encountered, and the size of the domain is determined by a force balance between the wall pressure and the "frictional force" of the nonzero wall coercivity. If the wall pressure is lower than this coercivity force, no movement will take place and the domain size will be stable. The stability condition can be expressed in terms of fields by dividing the forces in Eq. (2) by $4\pi R h|M(R)|$.

$$\left[\frac{\sigma_w(R)}{2R|M(R)|} + \frac{1}{2|M(R)|}\frac{\partial\sigma_w(R)}{\partial R} - \overline{H}_d(R) - H_a\right] \leq H_c(R). \quad (4)$$

Since no sign is attributed to the coercivity, we implicitly assume that only the absolute magnitude of the left-hand bracket is used in determining the regions of stability, and its sign indicates whether the wall pressure tends to expand or compress the domain.

The regions of stability for various temperature profiles and material parameters have been calculated on a computer using Eq. (4). Since the intrinsic magnetization may become zero if a ferrimagnetic material is heated through the compensation temperature, or if a ferromagnet is heated above the Curie temperature, we must

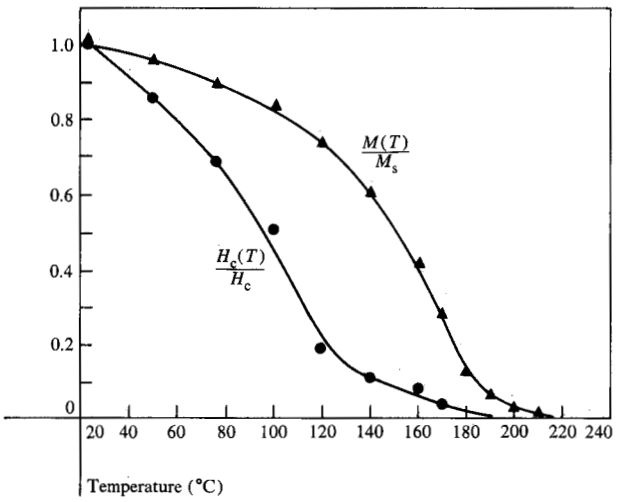

Figure 1 Variation of normalized magnetization and coercivity with temperature. The data are normalized to the room-temperature values and are typical of ferromagnetic MnAlGe films in the 500- to 800-Å thickness range.

be careful not to divide by zero in the computations. Therefore, we multiply Eq. (4) by $|M(R)|$ and solve for regions of stable radii in units of energy per unit volume:

$$\left[\frac{\sigma_w(R)}{2R}+\frac{1}{2}\frac{\partial\sigma_w(R)}{\partial R}-|M(R)|H_d-|M(R)|H_a\right] \leq |M(R)|H_c(R). \quad (5)$$

A Gaussian temperature profile with variance δ,

$$T(r)=T_a+(T_{max}-T_a)\exp-(r/\delta)^2, \quad (6)$$

is assumed present at some instant of time. The corresponding radial distributions of magnetization and coercivity are derived by combining this temperature profile with measured data of $M(T)$ and $H_c(T)$. Typical data for ferromagnetic, polycrystalline MnAlGe are shown in Fig. 1. These data were tabulated and entered as input into the computer, and the values of M and H_c for a specific temperature (and radius) were derived by linear interpolation.

To calculate σ_w, and $\partial\sigma_w/\partial R$, we make use of the function

$$\sigma_w=4(K_uA)^{\frac{1}{2}}, \quad (7)$$

where K_u is the uniaxial anisotropy constant and A is the exchange constant. It has been shown that for a wide range of temperatures in a uniaxial ferromagnet the anisotropy constant is related to the magnetization, to first order, by a third-power dependence [9]:

$$K_u=K_u^0[M(T)/M(T_a)]^3. \quad (8)$$

The simplest assumption for the variation of the exchange constant with magnetization is a second-power dependence [10]. Thus the final expression for wall energy becomes

$$\sigma_w(M)=\sigma_w^0[M(T)/M(T_a)]^{\frac{5}{2}}. \quad (9)$$

where σ_w^0 is the value of wall energy in the absence of the temperature distribution. Since the radial distributions for magnetization are known from the tabulated data and the temperature profile, we can calculate the value of σ_w at any radius and use numerical methods to compute $\partial\sigma_w/\partial R$. For the specific case considered below, $\partial\sigma_w/\partial R$ always acts to shrink the reversed domain.

Equation (11) is applicable to a ferromagnet heated to the Curie point. For a ferrimagnet we make the simplifying assumption that the compensation temperature (and the maximum temperatures represented by the temperature profile) is much lower than the Curie temperature. Therefore, the anisotropy and exchange constants are taken to be independent of the net magnetization for a range of temperatures near the compensation point:

$$\sigma_w=\text{constant};$$
$$\partial\sigma_w/\partial R=0. \quad (10)$$

This assumption would not be valid if the magnetization of the sublattice which controls the anisotropy were not independent of temperature in the vicinity of T_{comp}.

Numerical calculations

Ferromagnetic case

First we consider a ferromagnetic material. The dependencies of coercivity and magnetization on temperature used in the model are shown in Fig. 1 and are representative of the magneto-optical material MnAlGe. A Gaussian temperature profile with a peak temperature of 440 °C was considered to illustrate the situation where the Curie temperature (≈200°) was exceeded. The following parameters were also used [11]:

$$\sigma_w^0=1.0\ \text{erg/cm}^2\ (10^{-3}\ \text{J/m}^2),$$
$$M(T_a)=175\ \text{emu/cm}^3\ (2.2\times10^{-1}\ \text{W/m}^2),$$
$$H_c(T_a)=3125\ \text{Oe}\ (2.5\times10^5\ \text{A/m}),$$
$$H_a=500\ \text{Oe}\ (4\times10^4\ \text{A/m}),\ \text{and}$$
$$h=800\ \text{Å}.$$

Figure 2(a) shows the various terms in Eq. (5) for domain radii up to 6 μm. The temperature and magnetization profiles are also shown in Fig. 2(b). Note that the demagnetizing term and the term involving the applied

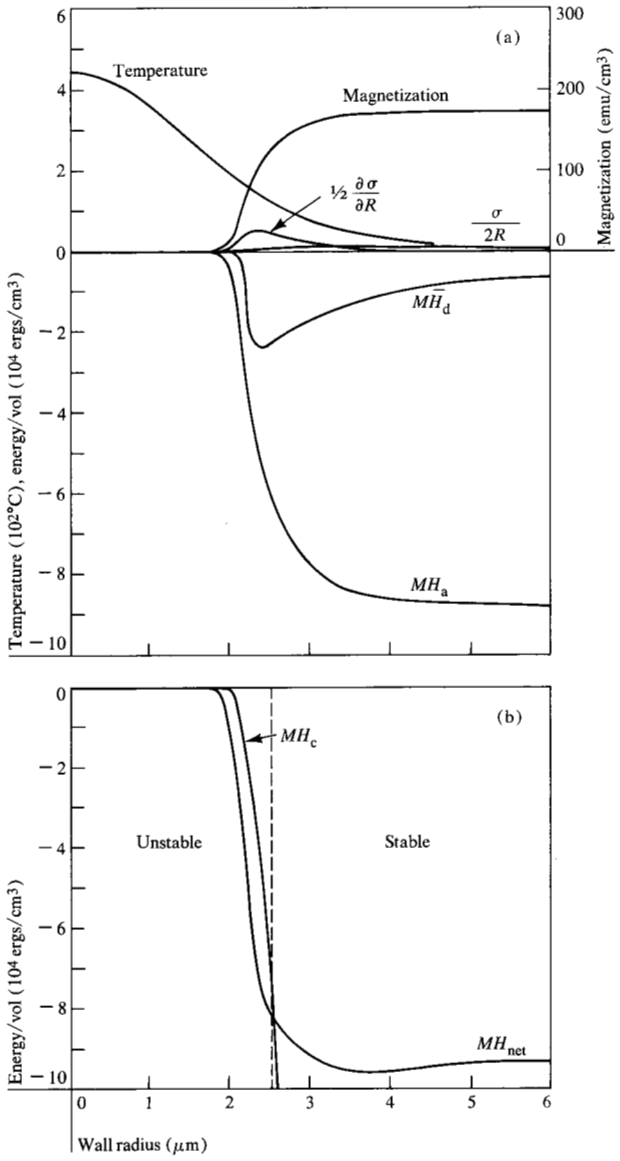

Figure 2 Plot of the terms in Eq. (5) for a ferromagnetic material. The peak temperature was 440 °C. (a) Curves showing both the temperature and magnetization profiles. Part of the film is above the Curie point and M is reduced to zero. (b) The sum of the left-hand terms of Eq. (5) is labeled MH_{net} and the intersection of this curve with MH_c determines the region of stable domain radii.

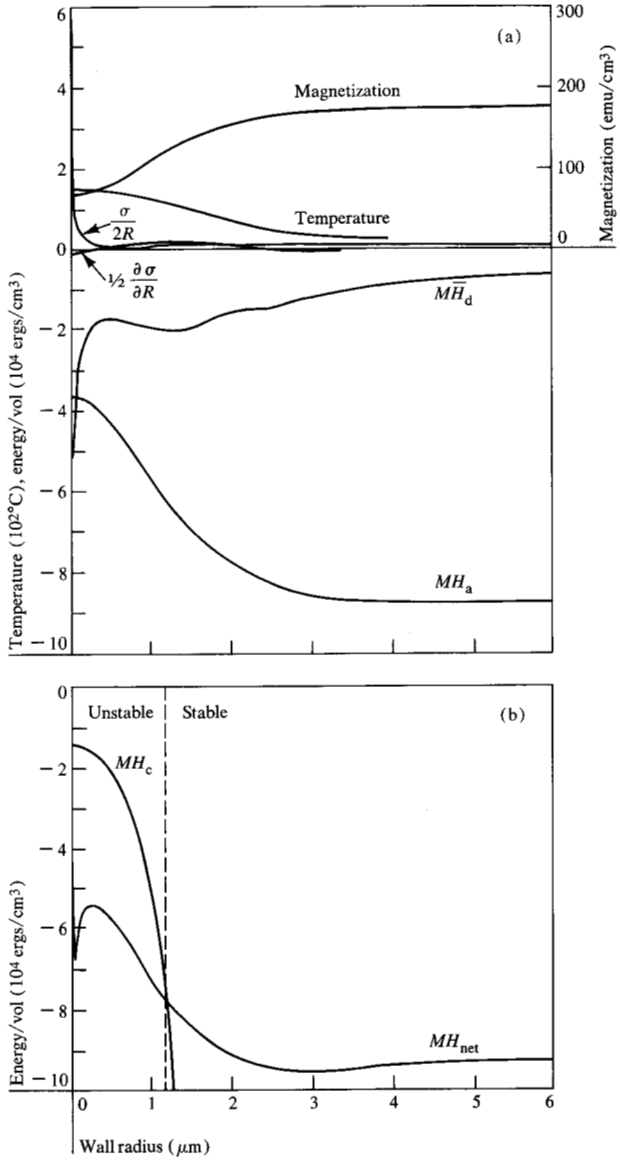

Figure 3 Plot of the terms in Eq. (5), similar to Figure 2, but for a peak temperature of 160 °C, which is below the Curie temperature.

external field are dominant. The positive terms involving the wall energy and its derivative represent forces that attempt to shrink the domain, and the negative terms represent expansive forces.

At the bottom of the figure, both the sum of the left-hand terms in Eq. (5), MH_{net}, and the coercivity term are plotted as functions of domain radius. The inequality of Eq. (5) is satisfied for all radii greater than the "critical radius" of 2.55 μm. This means that domains with radii greater than this value are stable, and domains with radii less than this critical radius will experience a net force greater than the local coercivity. In fact, the force will expand the domain until the force equals the coercivity at the critical radius, R_c, of 2.55 μm. It is interesting to note that the Curie point is exceeded only for radii less than 2.0 μm, but nucleated domains will grow to 2.55 μm and occupy regions of the film that are significantly below the Curie temperature. In the case of these calculations, the temperature at the critical radius, hereafter called the *critical radius temperature*, is only 122 °C.

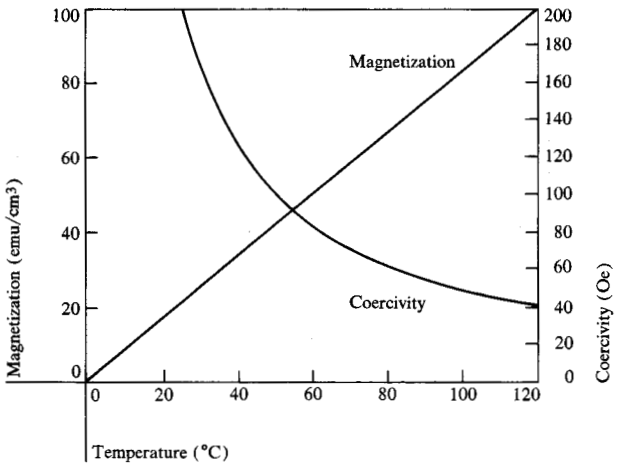

Figure 4 Variation of magnetization and coercivity with temperature for a ferrimagnetic material. The compensation temperature is 0 °C, and the coercivity is inversely proportional to the magnetization, i.e., $MH_c = 4000$ erg/cm^3.

Table 1 Calculations for MnAlGe, showing effect of external bias on critical radius and critical radius temperature.

Peak temp. (°C)	*Variance,* δ (μm)	*External bias,* H_a (Oe)	*Critical radius,* R_c (μm)	*Critical radius temp.* (°C)	*Coercivity at critical radius temp.* (Oe)
440	2.134	500	2.55	122	623
440	2.134	250	2.42	136	394
440	2.134	0	2.22	163	179

Table 2 Thermal profiles for determination of critical radii during a laser heating cycle up to 440 °C, for $H_a = 500$ Oe.

Time (ns)	*Peak temp.* (°C)	*Variance,* δ (μm)	*Critical radius* (μm)	*Critical radius temp.* (°C)
50	150	1.896	0.96	121
100	219	1.930	1.58	122
200	301	2.011	2.01	123
500	440	2.134	2.55	122
600	252	2.337	2.11	122
700	197	2.384	1.76	123

The situation with no portion of the film above the Curie temperature is shown in Fig. 3. A peak temperature of only 160° was used in the calculation, and the various terms are shown once again. The terms involving wall energy have a different behavior for very small radii, but the applied field and demagnetizing field terms still dominate for the material parameters considered. The critical radius of ≈1.2 μm is less than the previous case. It is most interesting to see, however, that the critical radius temperature is 122 °C, and is the same as that obtained for the previous temperature distribution. Calculations with other peak temperatures will yield a variety of critical radii at which a balance of forces occurs, but the critical radius temperature associated with these radii will be 122° (within ±2°).

The critical radius temperature, for the parameters used in the two examples, is controlled by the value of the external bias, H_a. The dominant energy term in the left-hand side of Eq. (5) is the one involving H_a, and the equation for the critical radius, R_c, reduces to $H_c(R_c) \approx H_a$. Thus, the critical radius temperature for the numerical examples could be estimated by using Fig. 1 to determine the temperature rise necessary to reduce the coercivity to 500 Oe. Accordingly, lower external biases imply higher critical radius temperatures.

These conclusions are further illustrated by the numerical results presented in Table 1. These calculated results not only indicate the error in the approximate solution given above, but show that the critical radius, R_c, increases with increasing external bias, as one intuitively expects.

To determine the critical radii at various times during a laser heating cycle, thermal profiles were determined numerically from a finite-difference solution to the heat equation. The laser was turned off after 500 ns, and the temperature distributions reflect heat flow into a semi-infinite substrate and radial flow in the magneto-optical film.

The temperature profiles were then used in the magnetic model and a set of critical radii and critical radius temperatures were determined from the quasistatic theory given above. These results are given in Table 2 for an external bias of 500 Oe.

During a laser pulse, the largest critical radius occurs at the instant of the largest temperature excursion. Thus, when a small domain is nucleated during the heating part of the cycle, it will continue to expand until the laser is turned off. In the example, the maximum temperature rise occurs at 500 ns, and the domain expands to 2.55 μm. As cooling begins, the critical radius becomes progressively smaller. Since domains with radii larger than the instantaneous critical radius are stable, the domain established at the moment of maximum temperature remains during the balance of the cooling part of the thermomagnetic writing cycle.

A very important question is the range of stable radii that exists when the film returns to ambient temperature and the external bias field used for writing is subsequently

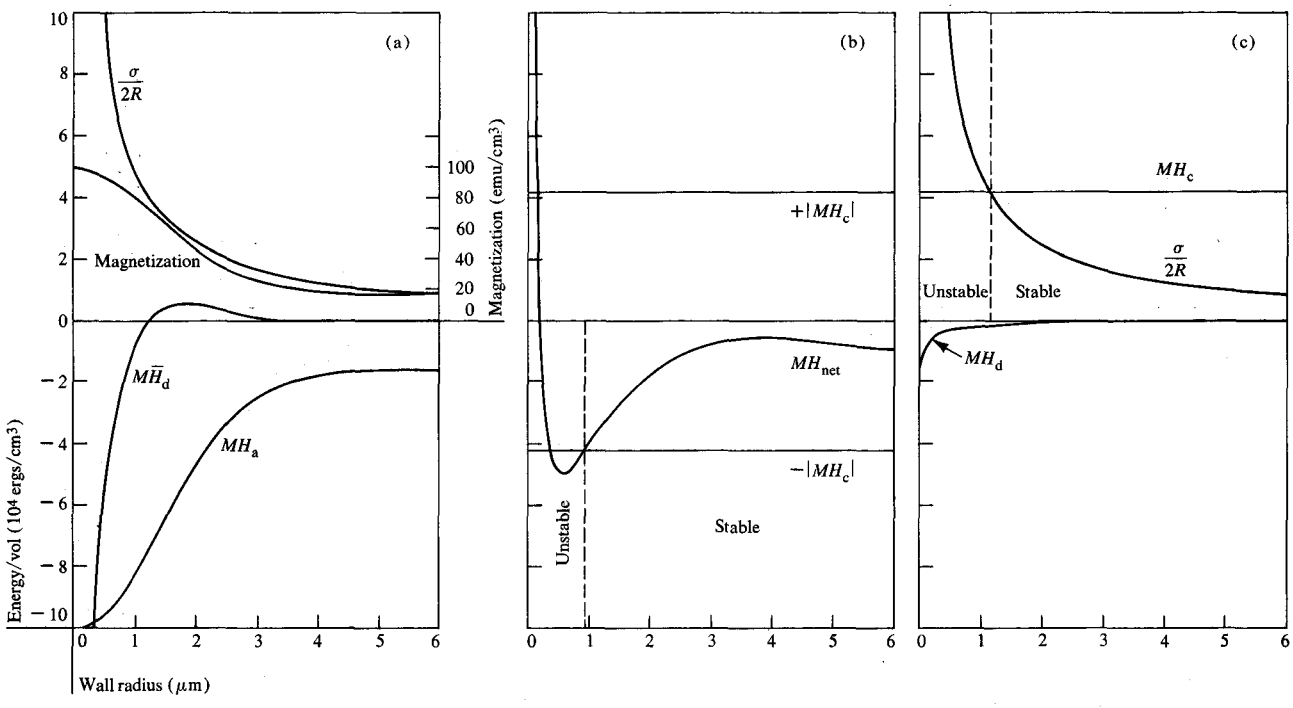

Figure 5 (a) Plot of the terms in Eq. (5) for a ferrimagnetic material. Parameters assumed in the calculation are given in the text. (b) Calculation with bias field $H_a = 100$ Oe and critical radius $R_c = 0.96$ μm. (c) Isothermal conditions with no external bias, $H_a = 0$ Oe. The selfmagnetostatic term is small in comparison to the wall-energy term, and $R_c = 1.16$ μm.

removed. It is conceivable that the presence of a bias and the thermal profile can produce a bit that is "conditionally" stable for a set of parameters and becomes unstable when those external factors are removed.

We may estimate the critical radius for the ferromagnetic case above for the condition in which there are no external influences. The largest value for the self-demagnetizing field is [4] $H_d = 4\pi M(T_a) = 2200$ G, and this value occurs for very small radii (i.e., $R \ll h$). When the coercivity and demagnetizing field are multiplied by $M(T_a)$, the equation for the critical radius becomes $\sigma_w/2R_c = 9.32 \times 10^5$, or $R_c = 7.5 \times 10^{-7}$ cm. This is much smaller than the critical radii calculated in Table 1, and the conclusion is that the bit whose writing was simulated by the calculations is not "conditionally" stable but persists even when the film is removed from the writing environment.

Although the question of conditional stability does not seem to be a critical one for the parameters associated with the ferromagnetic case, we now show that it becomes a central issue for ferrimagnetic materials having a compensation point.

• *Ferrimagnetic case*

Consider a ferrimagnetic material having a compensation temperature, T_{comp}. For numerical computations we use parameters typical of thin films of amorphous $GdCo_x$ ($x \approx 4$) [8], and we find that the stability and minimum radius of thermomagnetically written bits are influenced by the difference between the ambient and compensation temperatures (i.e., $\Delta T = T_a - T_{comp}$).

As a specific example, the functional dependencies of the magnetization and coercivity on temperature shown in Fig. 4 were used. These data are consistent with $T_{comp} = 0$ °C, $H_c = 5000/|T - T_{comp}|$, and $4\pi M = 10.6 \times |T - T_{comp}|$. The magnetization-coercive force product is a constant, independent of temperature, and is $MH_c = 4000$ erg/cm^3 (4×10^2 J/cm^3). The numerical results are indicated in Fig. 5 with the following additional parameters:

$\sigma_w = 1.0$ erg/cm^2 (10^{-3} J/m^2)

$\delta = 2.134$ μm

$h = 600$ Å

$T_a = 20$ °C

$T_{max} = 120$ °C

$H_a = 100$ Oe (8×10^3 A/m)

The results in Fig. 5(a), indicate that the critical radius of interest is $R_c = 0.96$ μm. Bits with radius R in the

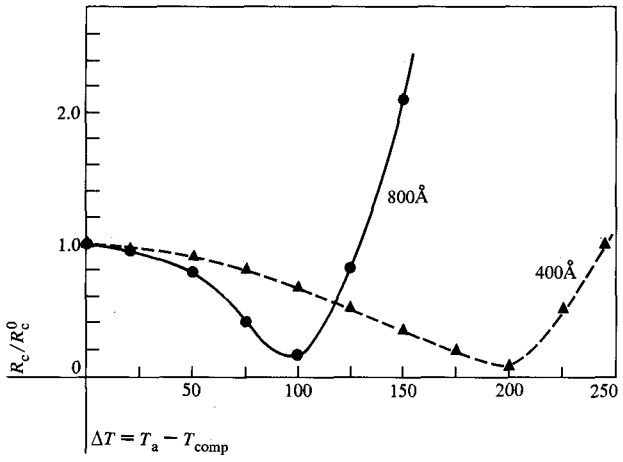

Figure 6 Minimum bit radius vs ΔT. The data points indicated are results of a simple bubble calculation on a film of constant temperature, T_a. When ΔT is small the forces on the bit are compressive and originate from the wall energy. When ΔT is large the forces originate from the selfmagnetostatic energy and tend to expand the bit. At intermediate values these two forces counteract one another and smaller stable bits can result.

range 0.36 μm $< R < R_c$ will expand until $R = R_c$, and bits with $R < 0.16$ μm will collapse and vanish. Bits in the region 0.16 μm $< R <$ 0.36 μm are considered quasi-stable because any perturbations which force the radius out of this range are not met with a restoring force, but will cause the bit to either vanish or expand to $R = R_c$. Of course, bits with $R > R_c$ are stable for the particular set of assumed parameters. If $T_{max} = 120$°C is the largest temperature applied during the thermomagnetic writing process, then $R_c = 0.96$ μm is the largest radius one expects during the heating cycle.

The question of whether the bit with $R = 0.96$ μm is stable or not after the film returns to the ambient temperature must now be examined. With the write bias $H_a =$ 100 Oe still applied to the film, calculations are obtained for $T_{max} = T_a = 20$ °C with the result $R_c' = 0.83$ μm. Since $R_c > R_c'$, the bit is still stable. In this case, however, M is only 17 emu/cm^3 (2.1×10^{-2} W/m^2), and the wall energy term dominates Eq. (5). Therefore, bits smaller than R_c' will collapse to zero radius.

When the external bias field is removed, i.e., $H_a = 0$, the critical radius becomes $R_c'' = 1.16$ μm, and the terms in Eq. (5) for this set of parameters are shown in Fig. 5(c). The wall-energy term clearly dominates, and now since $R_c < R_c''$ the bit is no longer stable and vanishes.

This example, in which a bit is established when $T_{max} =$ 120 °C, illustrates the situation referred to above as "conditional stability." Thus as long as certain, nonstandard conditions prevail (i.e., the maintainence of a writing bias) the bit is stable, but upon return to standard conditions of ambient temperature and no external fields, the bit becomes unstable. For the conditions present in this example, the instability causes the bit to collapse and vanish. We have observed this behavior in laboratory experiments with thin films of GdCo in which an external bias is required to maintain the presence of small thermomagnetically recorded bits. If the external writing bias is increased during recording, thereby enlarging the bits beyond a critical size, the reversed domains are retained when the sample is removed from the writing environment.

For $T_a = 20$ °C and the film parameters used, it can be seen from the results indicated in Fig. 5(c) that $R = 1.16$ μm is the smallest stable spot that can be thermomagnetically recorded. Any smaller bits eventually collapse under the influence of the wall energy.

In the conditionally stable case illustrated above, the external write-bias provides a force tending to expand the bit and counterbalances the collapsing force of the wall energy. As a result small bits can temporarily be stabilized. A similar counterbalancing force can be realized by increasing ΔT. This increases the demagnetizing field, H_d, arising from the self-magnetostatic energy because of the larger values of magnetization. Larger values of ΔT can be obtained either by increasing the ambient temperature, T_a, or by altering the compensation temperature, T_{comp}. For GdCo the compensation temperature can be conveniently controlled by adjustment of the preparation conditions [8]. In our calculations, however, it is more convenient to change T_a.

To investigate the minimum bit size for a range of ΔT it is necessary only to compute the critical radii for the isothermal case ($T = T_a$) with $H_a = 0$. The results of this calculation are given in Fig. 6 for films of 400 Å and 800 Å. As expected, $\Delta T \approx 0$ yields critical radii dominated by wall energy forces and can be calculated from $\sigma_w/2R_c^0 \approx MH_c = 4000$ ergs/cm^3, (4×10^2 J/m^3), or $R_c^0 \approx 1.25$ μm.

For larger ΔT, the counterbalancing effect of the self-magnetostatic energy term is increased and smaller bits are possible. If ΔT is increased to large values the self-magnetostatic term becomes dominant, with the result that recorded bits grow to unnecessarily large radii. Consequently, there is a value of ΔT between the two extremes that will support the smallest possible bit.

Another consequence of large ΔT has been observed in the laboratory. Bits recorded thermomagnetically in this regime show irregular, jagged boundaries, and in some extreme cases break up into multiple domains. On the other hand, bits written in the $\Delta T \approx 0$ regime generally exhibit smooth, regular boundaries. This effect is illustrated in the photographs of recorded bits shown in Fig. 5. In each of the three cases illustrated an attempt was made to write the smallest bits possible using a fo-

cused GaAs laser. The transition from smooth bits to irregularly shaped bits is quite clear, and the inability to write the smallest possible spots in the $\Delta T \approx 0$ regime is also indicated.

Summary and conclusions

Calculations have been performed to determine the stable radius of a cylindrically symmetric domain, or bit, nucleated during thermomagnetic writing with a laser beam. A ferromagnetic material with a second-order transition at the Curie temperature has been used as an example, and it was found that the temperatures existing at the critical radius, R_c, are less than the Curie temperature. The exact temperature value depends on the details of the variation of magnetization and coercivity with temperature and on the external bias. To first order, the critical radius temperature is the temperature necessary to reduce the coercive force to a value equal to the external bias. Higher biases, therefore, imply lower critical temperatures.

Finally, the largest critical radius occurs at the moment of maximum temperature rise. Since domains larger than the critical radius are stable, the largest domain established during the laser pulse will remain stable during the cooling of the material after the laser pulse is removed.

Calculations were also carried out for a ferrimagnetic material with a compensation point, $T_{comp} = 0$ °C. The regions of stability depend on ΔT, the difference between ambient and compensation temperatures. When $\Delta T \approx 0$, the magnetization is small, and the selfmagnetostatic forces have little effect. The wall-energy forces dominate and the critical radius, R_c^0, may be estimated from $R_c^0 = \sigma_w/(2MH_c)$. Bits with $R < R_c^0$ can be written in the presence of an external bias, but are considered conditionally stable because they collapse and vanish under the influence of the wall-energy forces when the bias is removed.

If ΔT is increased, the self-magnetostatic forces also increase and counteract the collapsing forces arising from the wall energy. In this regime of ΔT, the smallest bits may be written. We have observed, however, that when self-magnetostatic forces are important, the bits assume irregular shapes in order to minimize the total energy. With ΔT increased to still larger values, the self-magnetostatic energy dominates. Bits with $R < R_c$ are subject to an expanding force and grow until $R = R_c$. For sufficiently large ΔT, the bubble-type model used here fails because the bit breaks up into several domains consistent with a "minimum-energy" configuration.

For smooth-walled, well-defined bits, one should strive to write bits with $R_c > R_c^0 = \sigma_w/(2MH_c)$ and operate in the regime where wall energy dominates. In order to decrease R_c^0 in this regime (and thereby increase areal storage density) one may try to increase H_c by enhancing the uniaxial anisotropy [8], K. Any increase in K, however, will also increase the wall energy since $\sigma_w \propto \sqrt{K}$. Thus, R_c^0 will decrease only slowly with increasing anisotropy.

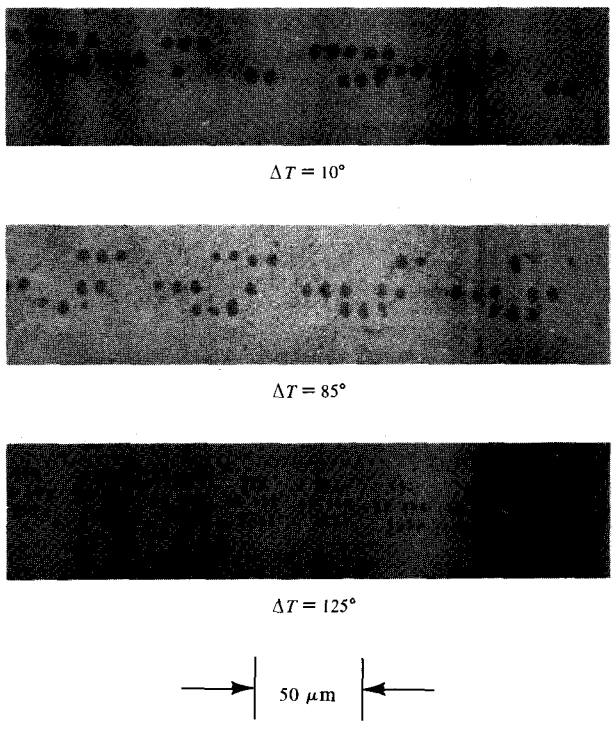

Figure 7 Thermomagnetically written bits on films of GdCo with different compensation temperatures. Minimum-size bits were written on films with $\Delta T = 10°$, 85°, and 125°, respectively, and the photographs show the appearance of the resulting reversed areas. The bits for $\Delta T = 125°$ do not represent the smallest possible bits but were limited by the size of the focused laser beam.

Acknowledgments

I thank D. Treves and K. Lee for many helpful discussions, R. Koepcke for help with the FORTRAN coding, E. Sawatzky for preparation of the GdCo samples, H. Wieder, B. R. Brown, D. Franich, and C. Stratton for results of their thermomagnetic writing experiments, and A. Juliana for design of the equipment. I also thank B. D. Silverman and C. F. Shelton for their interest in these calculations, and B. Argyle for a number of helpful suggestions on the manuscript.

Appendix A: Calculation of demagnetizing field

Consider a right-handed cylindrical coordinate system. A right-circular cylinder defines a domain with magnetization reversed within its boundaries, but with the magnitude of the magnetization permitted to be a radially symmetric function of space. The perpendicular component of magnetic field is calculated [12] from

$$H_\perp(r,\theta,z)=\int_{\text{Vol}}(-\mathbf{M}\cdot\mathbf{k}+3(\mathbf{M}\cdot\mathbf{r})\mathbf{r}\cdot\mathbf{k})/r_{12}^{\,3}, \quad \text{(A1)}$$

where

$$r_{12}^{\,2}=r^2+r'^2-2rr'\cos(\theta-\theta')+(z-z')^2$$

and $\mathbf{r}$ is a unit vector in the direction of r_{12}. Now,

$$\mathbf{r}\cdot\mathbf{k}=(\bar{r}_{12}/r_{12})\cdot\mathbf{k}=(z-z')/r_{12}$$

and the expression becomes

$$H_\perp(r,\theta,z)=\int_0^\infty\int_0^{2\pi}\int_0^h\left[-\frac{M(r')}{r_{12}^{\,3}}+\frac{3(z-z')^2M(r')}{r_{12}^{\,5}}\right]r'\,dr'\,d\theta'dz'. \quad \text{(A2)}$$

If we note that

$$\frac{d}{dz'}\left(\frac{z-z'}{r_{12}^{\,3}}\right)=-\frac{1}{r_{12}^{\,3}}+\frac{3(z-z')^2}{r_{12}^{\,5}} \quad \text{(A3)}$$

we can integrate over z', and we find

$$H_\perp(r,\theta,z)=\int_0^\infty\int_0^{2\pi}\frac{M(r')(z-h)r'dr'd\theta'}{[r^2+r'^2-2rr'\cos(\theta-\theta')+(z-h)^2]^{\frac{3}{2}}}-\int_0^\infty\int_0^{2\pi}\frac{M(r')zr'dr'd\theta'}{[r^2+r'^2-2rr'\cos(\theta-\theta')+z^2]^{\frac{3}{2}}}. \quad \text{(A4)}$$

Using the coordinate transformation $\gamma=\theta-\theta'$ and the integral identity

$$\int_0^{2\pi}\frac{d\gamma}{(a+b\cos\gamma)^{\frac{3}{2}}}=\frac{1}{(a^2-b^2)}\int_0^{2\pi}(a+b\cos\gamma)^{\frac{1}{2}}d\gamma \quad \text{(A5)}$$

we obtain, after some manipulation, the following expression for the field:

$$H_\perp(r,\theta,z)=4\int_0^\infty\frac{M(r')(z-h)E(\zeta)r'dr'}{[(r+r')^2+(z-h)^2][(r-r')^2+(z-h)^2]^{\frac{1}{2}}}-4\int_0^\infty\frac{M(r')zE(\xi)r'dr'}{[(r+r')^2+z^2][(r-r')^2+z^2]^{\frac{1}{2}}}, \quad \text{(A6)}$$

where

$$\zeta=\frac{4rr'}{[(r+r')^2+(z-h)^2]},$$

$$\xi=\frac{4rr'}{[(r+r')^2+z^2]},$$

and $E(x)$ is the complete elliptic integral of the second kind. This equation reduces to Bernal's [13] Eq. (13) when the field is evaluated in the plane $z=q=h/2$.

Appendix B: Evaluation of the derivative of the demagnetizing energy

The demagnetizing energy can be calculated from

$$E_d=\tfrac{1}{2}\int_0^\infty\int_0^{2\pi}\int_0^h M(r,\theta,z)\,H_\perp(r,\theta,z)rdrd\theta dz. \quad \text{(B1)}$$

For simplicity, consider only the *first* term in Eq. (A4) with the functional form of the magnetization $M(r,\theta,z)=-M_sf(r)[1-2u(R-r)]$. where M_s is the saturation value of magnetization,

$$u(x)\begin{cases}0, & x<0,\\ \equiv\tfrac{1}{2}, & x=0,\\ 1, & x>0,\end{cases}$$

$$|M(R)|\equiv M_sf(R).$$

The first term becomes

$$\tfrac{1}{2}\int_0^\infty\int_0^{2\pi}\int_0^\infty\int_0^{2\pi}\int_0^h\frac{M_s^2(z-h)f(r)[1-2u(R-r)]f(r')[1-2u(R-r')]rr'drd\theta dr'd\theta'dz}{[r^2+r'^2-2rr'\cos(\theta-\theta')+(z-h)^2]^{\frac{3}{2}}}. \quad \text{(B2)}$$

The derivative of Eq. (B2) with respect to the wall radius, $\partial E_d/\partial R$ yields

$$-M_s^2\int_0^\infty\int_0^{2\pi}\int_0^\infty\int_0^{2\pi}\int_0^h\left\{\frac{(z-h)f(r)[1-2u(R-r)]f(r')\delta(R-r')}{[r^2+r'^2-2rr'\cos(\theta-\theta')+(z-h)^2]^{\frac{3}{2}}}+\frac{(z-h)f(r)\delta(R-r)f(r')[1-2u(R-r')]}{[r^2+r'^2-2rr'\cos(\theta-\theta')+(z-h)^2]^{\frac{3}{2}}}\right\}\times rr'drd\theta dr'd\theta'dz. \quad \text{(B3)}$$

By splitting Eq. (B3) into two separate integrals, and integrating by the variable indicated in the argument of the respective Dirac-delta functions, and by recognizing the symmetry of the resulting parts with respect to r and r', one may recombine the two parts into

$$-2M_s^2Rf(R)\int_0^\infty\int_0^{2\pi}\int_0^{2\pi}\int_0^h\frac{(z-h)f(r')[1-2u(R-r')]r'dr'd\theta d\theta'dz}{[R^2+r'^2-2Rr'\cos(\theta-\theta')+(z-h)^2]^{\frac{3}{2}}}. \quad \text{(B4)}$$

Now when the coordinate transformation $(\theta,\theta')\rightarrow(\theta,\gamma)$ is made, with $\gamma=\theta-\theta'$ and after it is and integrated over θ, this expression becomes

$$- 4\pi M_s^2 \, Rf(R) \int_0^{\infty} \int_0^{2\pi} \int_0^{h}$$

$$\frac{(z-h) f(r')[1-2u(R-r')] r' dr' d\gamma dz}{[R^2 + r'^2 - 2Rr' \cos\gamma + (z-h)^2]^{\frac{3}{2}}}. \quad \text{(B5)}$$

Finally, by re-ordering the order of integration we obtain

$$[4\pi Rh|M(R)|] \frac{1}{h} \int_0^h dz \left\{ \int_0^{\infty} \int_0^{2\pi} \right.$$

$$\left. \frac{M(r', \theta, z)\ (z-h) r' dr' d\gamma}{[R^2 + r'^2 - 2Rr' \cos\gamma + (z-h)^2]^{\frac{3}{2}}} \right\}. \quad \text{(B6)}$$

The quantity in curly brackets can be recognized as the first term in the expression for the field [Eq. (A4)] evaluated at the wall radius, R. Thus, if we define $\overline{H}_d$ as the z-averaged demagnetizing field at the domain wall,

$$\partial E_d/\partial R = [4\pi Rh|M(R)|]\ 1/h \int_0^h H_{\perp}(R, z, \theta)\, dz;$$

$$\partial E_d/\partial R = 4\pi Rh|M(R)|\overline{H}_d. \quad \text{(B7)}$$

References

1. W. K. Unger and R. Rath, "Thermomagnetic Writing in Homogeneous MnBi Films," *IEEE Trans. Mag.* MAG-7, 885 (1971).
2. H. Wieder and R. A. Burn, "Direct Comparison of Thermal and Magnetic Profiles in 'Curie Point' Writing on MnGaGe Film," *J. Appl. Phys.* **44,** 1774 (1973).
3. B. G. Huth, G. T. Sincerbox, and C. E. Stratton, "Some Thermomagnetic Experiments on MnAlGe," Paper 19-4, 1973 INTERMAG Conference, Washington, D. C., April 24-27, 1973.
4. A. H. Bobeck, "Properties and Device Applications of Magnetic Domains in Orthoferrites," *Bell System Tech. J.* **46,** 1901 (1967); A. A. Thiele, "The Theory of Cylindrical Magnetic Domains," *Bell System Tech. J.* **48,** 3287 (1969).
5. S. Schuldt and D. Chen, "Wall Stability of Cylindrical (Bubble) Domains in Thin Films and Platelets," *J. Appl. Phys.* **42,** 1970 (1971).
6. S. Esho, S. Noguchi, Y. Ono, and M. Nagao, "Optimum Thickness of MnBi Films for Magneto-Optic Memory," Paper MB2. 1973 Topical Meeting on Optical Storage of Digital Data, March 19-21, 1973, Aspen, Colo.
7. K. Lee, E. Sawatzky, and J. C. Suits, "Preparation and Properties of Non-Stoichiometric MnAlGe Thin Films," *J. Appl. Phys.* **44,** 1756 (1973).
8. P. Chaudhari, J. J. Cuomo, and R. J. Gambino, "Amorphous Metallic Films for Bubble Domain Applications," *IBM J. Res. Develop.* **17,** 66 (1973), and "Amorphous Metallic Films for Magneto-Optic Applications," *Appl. Phys. Letters* **22,** 337 (1973).
9. W. J. Carry, Jr., "Temperature Dependence of Ferromagnetic Anisotropy," *J. Appl. Phys.* **24,** 436 (1958).
10. J. C. Slonczewski, IBM Thomas J. Watson Research Center, Yorktown Heights, New York, private communication.
11. All of the parameters here are measured except for σ_w^0. No measured values for the wall energy are available for MnAlGe, but one can safely estimate values in the range 1 erg/cm^2 to 10 erg/cm^2.
12. W. F. Brown, *Magnetostatic Principles in Ferromagnetism*, Interscience Publishers, New York, 1962, p. 21.
13. E. Bernal, "Mechanism of Curie-Point Writing in Thin Films of Manganese Bismuth," *J. Appl. Phys.* **42,** 3877 (1971).

Received August 8, 1973

The author is located at the IBM Research Division Laboratory, Monterey and Cottle Roads, San Jose, California 95114.